ISSN : 0974 - 7486 Volume 14 Issue 3

Materials Science

An Indian Journal

Full Paper

MSAIJ, 14(3), 2016 [067-076]

Experimental and thermodynamic study of chromium-base alloys containing nickel

Elodie Conrath*, Patrice Berthod
Institut Jean Lamour (UMR 7198), Team 206 "Surface and Interface, Chemical Reactivity of Materials"
Faculty of Science and Technologies, B.P. 70239, 54506 Vandœuvre-lès-Nancy, (FRANCE)
E-mail: elodie.conrath@univ-lorraine.fr, patrice.berthod@univ-lorraine.fr

ABSTRACT

The chromium-rich half part of the binary Cr-Ni system was explored by thermodynamic calculations and by the synthesis and the analysis of real alloys. Five Cr-xNi alloys with x=50, 40, 30, 20 and 10wt.% were cast, then exposed at 1200°C for 50 hours. Their as-cast and aged microstructures were characterized by X-ray diffraction, electronic microscopy and image analysis. Calculations were carried out with Thermo-Calc. Globally they are good correspondence between the microstructure results and the thermodynamic calculations in terms of mass fractions. The experimental data brought additional information about the morphology of the phases.

KEYWORDS

Cr-based alloys;
Cr-Ni binary system;
Thermodynamic calculation;
Foundry;
Microstructures.

INTRODUCTION

Chromium features among the most refractory metallic elements. Although its melting point close to 1900°C[1, 2] it is of course not so refractory as other metals like tantalum (3000°C) or tungsten (3400°C)[3], Cr is potentially interesting as possible base element for alloys devoted to applications at very high temperature. Chromium is additionally an interesting element for the resistance to hot oxidation since it forms a Cr_2O_3 oxide which contains only few defects (anionic or cationic interstitials or vacancies). This allows it acting as an efficient protective barrier isolating metal or alloy from the oxidizing atmospheres[4]. Consequently this element is present in rather high quantities (typically 10 to 30wt.%) in superalloys since several decades. Initially this was the case of the nickel-based and cobalt-based alloys[5,6] but now essentially in the last ones[7] because this is more aluminum which is present instead Cr in the actual high performance nickel-based superalloys[8]. Furthermore its rather low density (7.1 g/cm^3[3]), much lower than the Ta and W ones (16.6 and 19.3 g/cm^3 respectively[3]) and even a little lower than the cobalt and nickel ones (both 8.9 g/cm^3[3]), is interesting for the numerous applications in which centrifugal stresses exist in service.

Nickel is also one of the most used elements in very refractory alloys, but with a structural role. Even if in the past it was alloyed with 20 or 30wt.% of chromium in the first heat resistant alloys in the middle of the last century[5,6], nickel is now the most often alloyed with a long list of elements among which aluminum which forms γ'(Ni_3Al) precipitates very efficient to resist creep[7]. It can be also reinforced by carbides but the ones which are among the most mechanically efficient – TaC – are much less stable at high temperature in nickel-based alloys[9] than in the cobalt-based ones[10] or the iron-based ones[11,12].

Until today the association of these two elements in superalloys was essentially focused on the need of hot corrosion resistance but never on the potential gain in refractoriness. Thus, if the chromium content in nickel-based alloys was maintained at around 30wt.% maximum (always sufficient for efficiently combatting hot corrosion), much higher Cr contents were rarely envisaged, although 50 wt.%Cr and more may lead to enhanced creep resistance thanks to increases in fusion start temperature, by keeping of course good resistance to hot corrosion. Thus, new types of high temperature materials combining very high contents in chromium and the presence of a nickel-based phase (mechanical resistance and ductility at all temperatures thanks to its austenitic FCC crystalline network), may emerge. This makes the Cr-richest part of the chromium-nickel system of increased interest.

In this work five binary alloys, potentially devoted to use at high temperature in their present states or alloyed with minor elements, were selected: their names and wished chemical compositions are given in TABLE 1. They were subjected to preliminary thermodynamic calculations to know the natures and volume fractions which can be expected at high temperature, for example at 1200°C temperature already unattainable by the best actual superalloys for long-time service. They were thereafter synthesized foundry and their microstructures characterized. Additional thermodynamic calculations were thereafter carried out for each alloy for decreasing temperature to know the successive stable states as well as to better understand the development of the observed microstructures.

EXPERIMENTAL

Preliminary thermodynamic calculations

To anticipate in the knowledge of the possible difficulties which may be encountered to melt the alloys as well as their stable microstructures at high temperature a first set of calculations were carried out using Thermo-Calc[13]. On the one hand, the fusion temperature ranges of the compositions of interest were determined to assess the feasibility of the synthesis by foundry. On the other hand the stable metallurgical state corresponding to 1200°C was calculated for all compositions, to specify the natures of the present phases, their mass fractions and their contents in Ni and Cr.

Synthesis of the alloys

The five alloys were elaborated by high frequency induction foundry (CELES furnace, France) from small parts of pure elements: Cr and Ni, both >99.9wt.% in purity (suppliers: Delachaux for Cr and Eramet for Ni). In each case the parts were placed in a copper crucible internally cooled by fresh water circulation. A silica tube was placed surrounding the crucible and a copper induction coil (also cooled by internal water circulation) was placed around the silica tube isolating the crucible and the metallic parts from outside. Pumping until reaching about 0.03 millibars was realized three times, each time followed by introduction of pure argon until reaching about 800millibars. After final pumping, an atmosphere of 600 millibars of argon existed in the fusion chamber. The power was increasingly applied until reaching the temperature level demonstrated by the preliminary thermodynamic calculations as required for the fusion of nickel and chromium as well as for the steady molten state of the obtained liquid alloy. The power was maintained at this maximum during five minutes. This duration was identified by preliminary tests as compulsory to be sure to do not have any not melted parts of Ni or Cr for the average size of the used pure element parts (millimetric). This isothermal stage was followed by cooling, the rate of which was defined by the rate of power decrease. This procedure led to five ingots of a compact shape and weighing about 40 grams each.

Microstructure characterization

TABLE 1 : Designation and chemical compositions of the studied alloys (in weight percent)

Names given to the alloys	CN1	CN2	CN3	CN4	CN5
Compositions (1-x) Cr + xNi	x = 0.1	x = 0.2	x = 0.3	x = 0.4	x = 0.5

The ingots were cut using a Delta Buelher saw. A part from each of them was embedded in a cold resin mixture (resin CY230 and hardener HY956 from ESCIL, France). The mounted samples were thereafter ground with SiC papers, for grade varying from 80 to 4000. They were cleaned using ultrasonic vibrations in ethanol. Final polishing was realized using a non-woven textile disk enriched in 0.4µm silica particles (OPS, Struers), until obtaining a mirror-like state.

The alloys were first analyzed by X-Ray Diffraction (XRD, Philips X'Pert Pro diffractometer) then observed by Scanning Electron Microscopy (SEM, JEOL JSM-6010A) in Back scattered Electrons Shadow image (BES). The general chemical composition of the alloys was verified by Energy Dispersion Spectrometry (EDS) using the EDS device equipping the SEM. Spot EDS measurements were additionally carried out to specify the chemical compositions of the present phases.

To finish the microstructure characterization was completed by the measurements of the surface fractions of the phases using the image analysis tool of the Photoshop CS software (Adobe). When it was possible to suppose that the volume fractions were probably close to the measured surface fractions, these fractions were converted in mass fractions according to the following equation:

$$\mathbf{f_w}\left[\phi_j\right] = (\rho_{\phi j} \times \mathbf{f_v}\left[\phi j\right]) / \sum_i (\rho_{\phi i} \times \mathbf{f_v}\left[\phi i\right])$$

in which fw [φ_j], fv [φ_j] and $\rho\varphi_j$ are respectively the weight fraction, the volume fraction and the density of the phase φ_j. The values taken for the densities were 7.1 g cm^{-3} for the Body Centered Cubic (BCC) chromium-rich phase and 8.9 g cm^{-3} for the Face Centered Cubic (FCC) nickel-rich phase when they were present.

Additional thermodynamic calculations

To better understand how the observed microstructures were obtained new thermodynamic calculations were carried out again for the five compositions. The microstructural states of each alloy were computed every 50°C in the mushy state and every 100°C in the solid state down to 427°C. The appearance or disappearance of the phases and the evolutions of their theoretic fractions and compositions were thus deduced.

RESULTS AND DISCUSSION

Preliminary thermodynamic calculations

First the binary Cr-Ni diagram was computed to have a rapid look to the Cr-Ni system (Figure 1). The diagram is a very classical one, with a eutectic plateau and a middle area where two phases exist together.

As shown in the first line of results in TABLE 2 the calculated theoretic maximum liquidus temperature among the five alloys is logically the one of the chromium-richest alloy CN1, while the CN4's and CN5's ones are respectively 350°C and 450°C under. This very high temperature (≈1800°C) risks to lead to difficult melting during the elaboration of the chromium-richest alloys. Solidification ought starting with the crystallization of a chromium-based BCC phase for the four chromium-richest alloys (CN1 to CN4) while this is nickel austenite (FCC phase) which ought appears first in the case of the CN5 alloy (TABLE 3, first results line).

The calculated theoretic solidus temperatures, presented in the second results line of TABLE 2, are also very high, with the highest value for the CN1 alloy again (≈1650°C), comparable to the one of the famous intermetallic compound NiAl (which is unfortunately too brittle at room temperature and paradoxically too weak in high temperature creep). The solidus temperature decreases down to the eutectic one (≈1345°C) for the two nickel-richest alloys (CN4 and CN5). At the end of solidification (second results line in TABLE 3), the three chromium-richest alloys ought to be single-phased (BCC chromium-based phase with all Ni in solid solution, i.e. 10 to 30wt.%Ni from CN1 to CN3) while the two chromium-poorest alloys ought to be double-phased BCC+FCC, with principally BCC Cr saturated by 39wt.%Ni) in CN4 and principally FCC Ni saturated by 47wt.%Cr).

The third line of TABLE 3 shows the theoretic stable metallurgical states of the five alloys at 1200°C: still single-phased for CN1 and CN2, and double-phased BCC Cr(Ni) and FCC Ni(Cr) for the following alloys: mainly BCC Cr (saturated by almost 30wt.%Ni) for CN3, half part of the same BCC

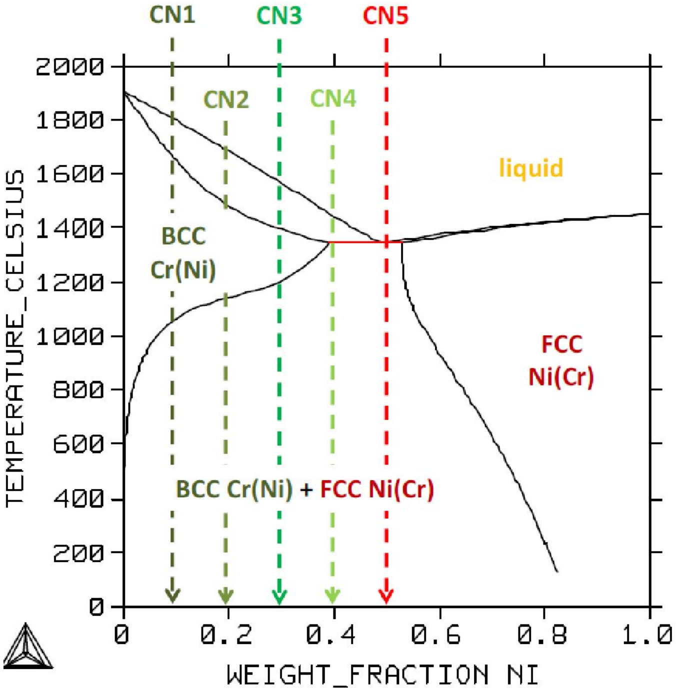

Figure 1 : The Cr-Ni diagram computed with Thermo-Calc[13]

TABLE 2 : Calculated temperatures of liquidus and solidus (Thermo-Calc[13])

alloys	CN1	CN2	CN3	CN4	CN5
$T_{liquidus}$ (K)	2071	1958	1839	1716	1621
$T_{solidus}$ (K)	1922	1754	1667	1618	1618

TABLE 3 : Microstructure states at Tliq, Tsol and 1473.15K (1200°C), according to Thermo-Calc[13] (mass.% phase; wt.%Cr or Ni in phase)

Alloys	CN1	CN2	CN3	CN4	CN5
at $T_{liquidus}$ (appearing solid)	BCC Cr-3.90Ni	BCC Cr-8.43Ni	BCC Cr-14.20Ni	BCC Cr-23.66Ni	FCC Ni-46.15Cr
at $T_{solidus}$	100% BCC Cr-10Ni	100% BCC Cr-20Ni	100% BCC Cr-30Ni	93.4% BCC Cr-39.08Ni + 6.6% FCC Ni-46.98Cr	78.4% FCC Ni-46.98Cr + 21.6% BCC Cr-39.08Ni
At 1200°C	100% BCC Cr-10Ni	100% BCC Cr-20Ni	97.8% BCC Cr-29.48Ni + 2.18% FCC Ni-46.54Cr	56.1% BCC Cr-29.48Ni + 43.9% FCC Ni-46.54Cr	85.6% FCC Ni-46.54Cr + 14.4% BCC Cr-29.48Ni

Cr solid solution and half part of the FCC Ni (saturated by 47wt.%Cr) for CN4, and mainly FCC Ni solid solution for CN5.

Microstructures of the obtained alloys

Despite the very high melting points of some of these alloys, all elaborations were successful. No unmelted particles were detected on the surfaces of the sectioned parts of the ingots. The obtained chemical compositions, shown in TABLE 4, are very close to the wished ones.

The microstructures of the obtained alloys as observed at ×250 with the SEM in BES mode are displayed in Figure 2. Despite the different grey levels which are visible on the corresponding SEM/BES micrographs the alloys CN1 and CN2 are single-phased: the single solid phase is the BCC chromium-based one, as confirmed by X-ray diffraction (XRD).

TABLE 4 : Microstructure states at Tliq, Tsol and 1473.15K (1200°C), according to Thermo-Calc[13] (mass.% phase; wt.%Cr or Ni in phase)

Names given to the alloys	CN1	CN2	CN3	CN4	CN5
Wished compositions Cr - Ni	89.8 – 10.2	80.0 – 20.0	69.9 – 30.1	60.0 – 40.0	50.0 – 50.0

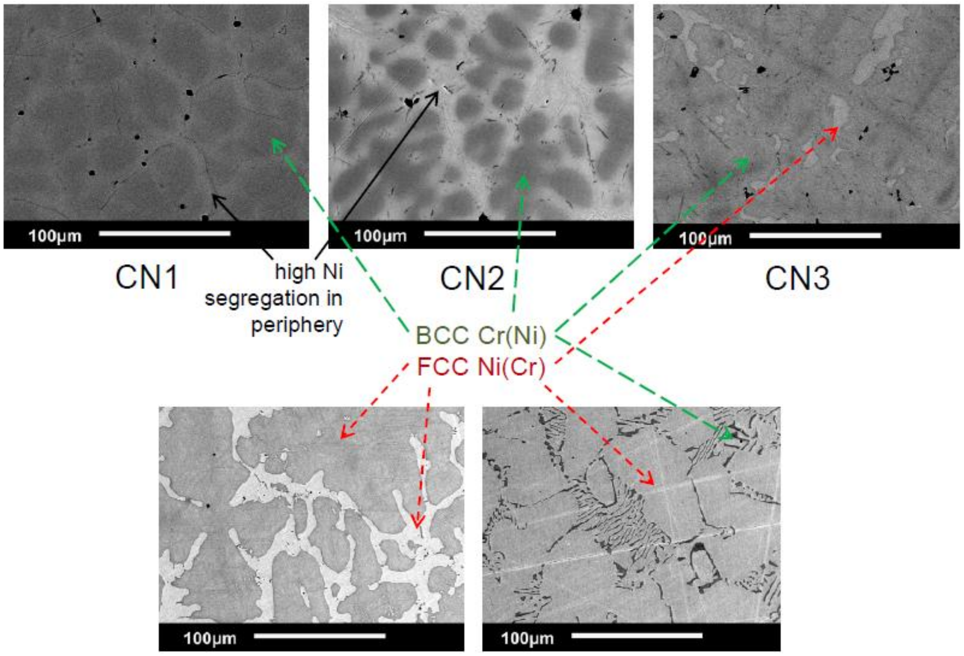

Figure 2 : Microstructures of the five alloys (SEM micrographs taken in BES mode)

Indeed there is not marked separation between the dark areas and the pale ones. By looking at higher magnification the transition from dark to pale is progressive (diffuse). As revealed by spot EDS analysis in the CN1 alloy, this results in an increase in local nickel content from the grain center (about 5wt%Ni) to the periphery (about 20 wt.%Ni). In the case of the CN2 alloy, the nickel content increases from about 10wt.% (grain center) up to 37wt.% close to the grain boundaries.

The nickel-richer alloys CN3 and CN4 alloys are, in contrast, really double-phased as also confirmed by XRD. The average composition of the dark phase (BCC chromium-based) is about Cr(bal.)-22.4wt.%Ni for the CN3 alloy and Cr(bal.)-34.9wt.%Ni for the CN4 alloy, while the average composition of the pale phase (FCC nickel-based) is about Ni(bal.)-66.2wt.%Cr for the CN3 alloy and Ni(bal.)-50.2wt.%Cr for the CN4 alloy.

The last alloy, CN5, is also double-phased but with a very different morphologies of the phases. The pale phase, FCC nickel-based containing 47.7wt.%Cr is dendritic while the dark phase, BCC chromium-based containing 30.5wt.%Ni, is mixed with the FCC matrix as a lamellar compound in the interdendritic spaces. The surface fractions of the present phases, issued from image analysis using Photoshop CS, are given in TABLE 5.

Calculations for the description of the microstructures' development

Despite that all the five alloys were expected being double-phased at room temperature, as suggested by Figure 1, two of them were single-phased. In addition, significant segregation phenomena were revealed by the BES micrographs and confirmed by EDS measurements. Additional calculations were carried out for the five alloys at different levels of temperatures regularly spaced from the liquidus temperature and 427°C, temperature under which no further solid state transformation maybe expected for reasons of too slow diffusion.

This was done for the five alloys but the case of only three of them will be presented here: CN1 representing in Figure 3 the case of a chromium-based alloy obtained as single-phased in its as cast-condition (CN1 and CN2), CN4 representing in Figure 4

TABLE 5 : Average surface fractions of the phases present in the alloys (%)

Names given to the alloys	CN1	CN2	CN3	CN4	CN5
BCC Cr-based phase	100	100	95	72	8
FCC Ni-based phase	/	/	5	28	92

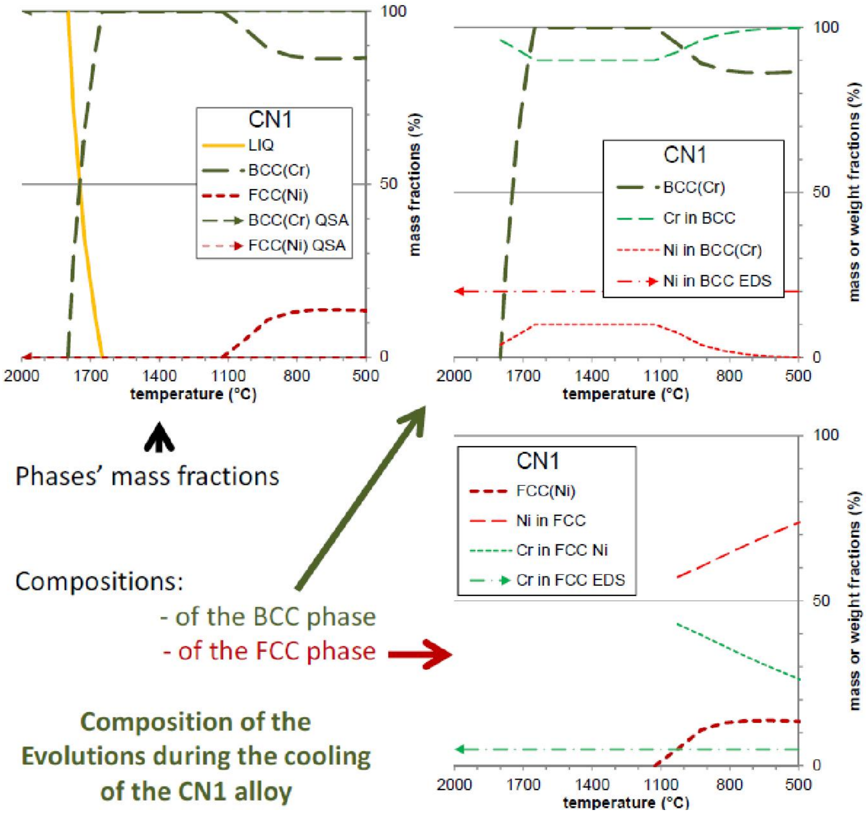

Figure 3 : Thermo-Calc calculations describing the solidification and solid state cooling of one of the alloys observed as-cast as being single-phased (here: the Cr-richest CN1 alloy)

the case of a chromium-based alloy obtained as double-phased (CN3 and CN4), and the case of the single Ni-based alloy of this study, CN5, in Figure 5.

As shown by the first graph of Figure 3 (left side) the BCC chromium-based phase is effectively the first solid phase to appear in the case of CN1 (and of CN2). During solidification, the nickel content in this BCC Cr-based phase increases from about 3.9 to 10 wt.%Ni (from about 8.4 to 20 wt.%Ni for CN2) while the nickel content in the liquid also increases but from 10 to 23.1 wt.%Ni (from 20 to 63.1 wt.%Ni for CN2).

Thereafter the BCC chromium-based solid remains the only phase existing during the solid state cooling down to about 1150°C (for CN2 too), with a Ni content evidently staying at 10 wt.% (20wt.% for CN2). Thereafter the FCC nickel-based phase should appear and grow until reaching 13 to 14 mass.% (28 to 29mass.% for CN2). The Ni content in the BCC chromium-based phase decreased then from 10 to 0.04 wt.% (20 to 0.04wt.%Cr for CN2) at 427°C while the chromium content in the FCC nickel-based phase decreases from 42.8 down to 24.4 wt.% (45.5 to 24.4wt.% for CN2) at 427°C.

The first graph of Figure 4 (left side) shows that this is the BCC chromium-based phase again which is the first solid to precipitate from the melt, for CN4 (and CN3). During solidification the nickel content in this BCC phase increases here too, from 23.6 to 39wt.%Ni (3.9 to 30wt.% Ni for CN3). At the same time the nickel content in the liquid increases from 40 to 49 wt.% in CN4 (decreases from 30 to 23.1 wt.% in CN3). In contrast with the two first alloys CN1 and CN2) solidification finishes with the precipitation of two phases, a BCC chromium-based one (leading to finally 93.4 mass.%, and a FCC nickel-based one (6.6 mass.%).

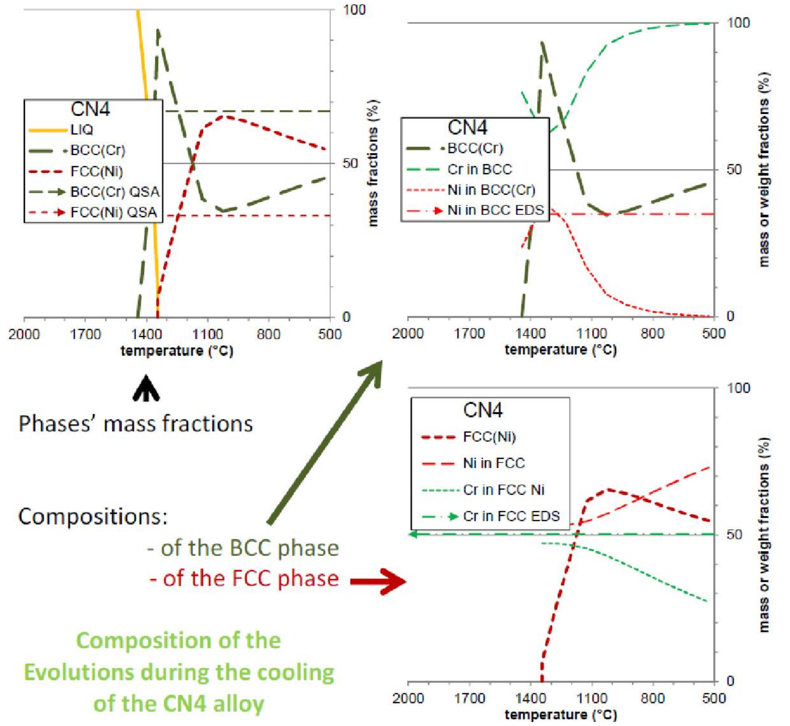

Figure 4 : Thermo-Calc calculations describing the solidification and solid state cooling of one of the chromium-based alloys observed as-cast as being double-phased (here: the Cr-richest CN4 alloy)

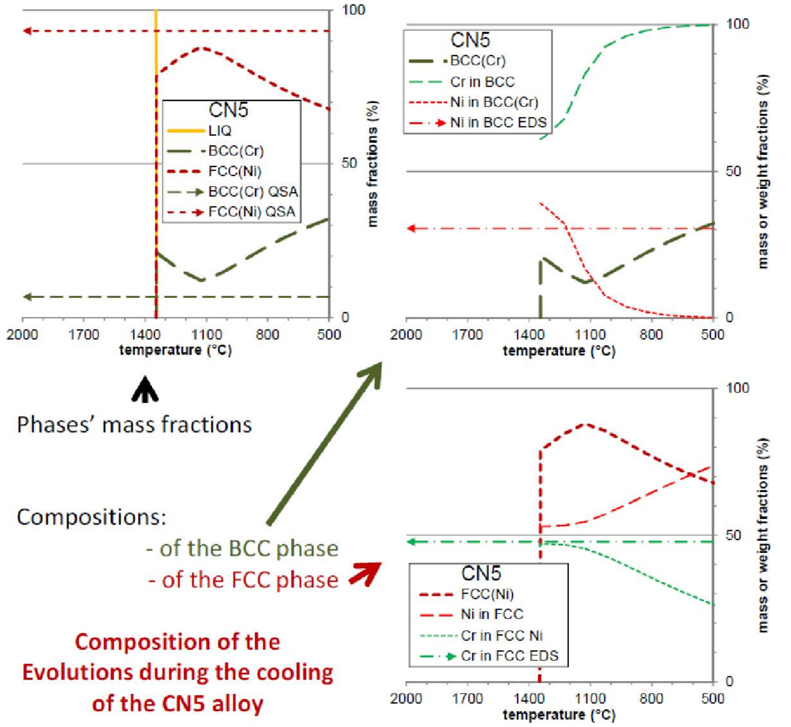

Figure 5 : Thermo-Calc calculations describing the solidification and solid state cooling of the double-phased CN5 alloy

In contrast the CN3 alloy ought to finish solidifying with only the BCC chromium-based phase, the FCC nickel-based one appearing after a solid state cooling down to 1227°C. After solidification the Ni content in the BCC chromium-based phase decreases continuously (but faster then slower) from 39 to 0.04wt.% (30 to 0.04wt.%Ni for CN3 only after the appearance of the FCC nickel-based phase).

The case of the CN5 alloy is totally different from the previous ones (Figure 5). Indeed solidification ought to start with the crystallization of the FCC nickel-based phase (containing initially 46.2 wt.%Cr) and finishes, as for the CN4 alloy, by a eutectic part in containing a 39wt.%Ni-containing BCC chromium-rich phase. At the end of solidification (1345°C) the alloy ought contain 78.4 mass.% of 47wt.%Cr-containing FCC nickel-based phase and 21.6 mass.% of 39.1wt.%Ni-containing BCC chromium-based phase. During cooling the mass fraction and Cr content of the FCC nickel-based phase vary: slight increase then slight decrease for its mass fraction and regular decrease from 47 to 24.4wt.% at 427°C for its Cr content. At the same time the mass fraction of the BCC chromium-based phase decreases then increases and its Ni content decreases until 0.04 wt.% at 427°C.

Comparisons between successive calculations and the as-cast alloys

For the CN1 alloy, which was seemingly single-phased in its as-cast condition, the EDS measurements showed that the Ni contents increased from about 5 in the grain centers to about 20 wt.% in periphery. These values are rather close to respectively the Ni content in the first appearing BCC crystals at solidification (4 wt.%Ni) and the final Ni contents in the liquid just before its final disappearance at the end of solidification (23 wt.%Ni), calculated with Thermo-Calc. This was observed again for the CN2 alloy: the 10wt.%Ni measured with EDS in the grains centers and the 37wt.%Ni measured in grain periphery are also rather close to the 9wt.%Ni of the first BCC crystals to appear and the 63wt.%Ni of the last disappearing liquid, respectively. In both cases the cooling was thus too fast to allow constant chemical homogenization of the growing BCC phase during solidification, with as results the intense chemical segregations which were evidenced in the metallographic samples of the as-cast CN1 and CN2 alloys. One can underline that, despite the great periphery nickel enrichment the FCC nickel-based phase did not succeed appearing. Dotted arrows are added to the two graphs present on the right of Figure 3 (CN1) to materialize the position of the EDS values of the Ni content in the BCC Cr-based phase (grain center) and of the Cr content in what ought to be the FCC Ni-based phase but which does not exists (periphery of BCC Cr-based grains only). This facilitates the comparisons between measured contents and calculated contents for the same locations.

For the CN4 alloy, as illustrated by the arrows added in the two graphs presented on the right side of Figure 4 there is a rather good correspondence between the measured Ni content in the BCC chromium-based phase and the calculated one for temperatures close to the end of solidification 34.9wt.%Ni (EDS) H” 35.6wt.%Ni (Thermo-Calc for 1227°C). This was also true for CN, with 22.4wt.%Ni (EDS) H” 30 to 16.8wt.%Ni (Thermo-Calc for 1227 to 1127°C). For CN4 again, the 50.2wt.%Cr measured in the FCC is close to the 47wt.%Cr calculated for the FCC nickel-based phase for 1345°C (almost the solidus temperature). However, concerning the CN3 alloy the 66.2wt.%Cr measured in the FCC nickel-based phase are significantly higher than the calculated one (45.4wt.%Cr at 1127°C furthermore decreasing to 24.4wt.%Cr at 427°C). Since these two alloys were double-phased in their as-cast states the surface fractions of the two phases were measured by image analysis, which allowed comparisons. The morphologies of these phases, which were neither acicular nor oriented, let think that the volume fractions were probably close to the surface fractions. This was what was supposed and the values (TABLE 5) were then converted into mass fractions according to equation (1). This led to 67 mass.% of BCC chromium-based phase and 33 mass.% of FCC nickel-based phase for CN4 (94 and 6 mass.% for CN3). These values led to the dotted arrows in the first graph of Figure 4 (left side) which allows seeing that the better correspondence was found between 1277 and 1227°C for CN4 (just under 1227°C for CN3). In contrast the mass fractions calculated for lower temperatures are much farer from the measured ones.

In the case of the CN5 alloy too it was possible to compare the chemical compositions of the two phases measured by EDS and their surface fractions converted into mass fractions to the corresponding calculated results. Concerning the mass fractions the ones issued from the surface fractions obtained from image analysis of SEM/BES micrographs, there was no exact correspondence but the measured (room temperature) and calculated data rather well fitted for calculations near 1127°C (Figure 5, arrows in the first graph on the left): at this temperature the calculated mass fractions are 88 and 12 mass.% of FCC nickel-based phase and BCC chromium-based phase, rather close to the experimental ones of 93 and 7 mass.% issued from conversion of the image analysis results. Concerning the chemical compositions of the phases, calculations at 1227°C led to 32.1wt.%Ni in the BCC chromium-based phase and 46.8wt.%Cr in the FCC nickel-based phase which are close to the 30.5wt.%Ni and 47.7 wt.%Cr in Ni measured by EDS.

General commentaries

Despite the very high temperatures of melting suggested by the preliminary calculations the five alloys were successfully elaborated, without any not melted parts of pure element, even the CN1 alloy that one may think as being especially difficult to obtain. This was possible thanks to the use of a high frequency induction melting, while this should be probably much more difficult with a more classical resistive furnace. In contrast, it was not possible to measure the temperatures of fusion and solidification start and end by differential thermal analysis since the melting temperature ranges were too high for usual apparatus.

Thus, alloys, chemically homogeneous at the ingot scale were obtained and their microstructures characterized. XRD diffractograms clearly showed that only two phase were present, the BCC chromium-based one and the FCC nickel-based one. Thus the rather fast cooling did not lead seemingly to additional metastable phase. With a maximum of two phases the thermodynamic system was respected. The comparison, in terms of number of the phases, their chemical compositions and their volume or mass fractions chemical homogeneity, between the obtained microstructures and the successive calculated equilibrium for decreasing temperature, showed that the five alloys did not respect these equilibrium during their cooling. In fact, the obtained microstructures in the as-cast alloys are globally the ones existing just after solidification, or only several tens degrees under. The two chromium-richest alloys CN1 and CN2 finished their solidification by becoming single-phased (BCC chromium-based phase), a state that they kept during the whole cooling down to room temperature. The nickel positive segregation occurred during solidification remained almost unchanged and, despite the very high concentration of nickel (50 wt.% or more) in the periphery of the BCC chromium-based grains, no external transformation into FCC phase occurred during the cooling. The cooling rate did not allowed nucleation and growth of this second phase which was furthermore compulsory according to the stable equilibrium at less than 1100°C.

In contrast the two phases obviously existed in the real CN3 and CN4 alloys, the FCC nickel-based phase necessarily appeared by solid state transformation during cooling in the CN3 alloy, and at the end of solidification for the CN4 alloy. The CN5 alloy was also double-phased but with now a solidification starting with the FCC nickel-based phase, the BCC chromium-rich one appearing at the end of solidification, when the eutectic part of solidification happened. However, in these three last cases, the microstructures, in terms of both mass fractions and chemical compositions of the present phases, clearly correspond to the ones which existed at very high temperature, soon after the end of solidification. They do not correspond to the phase equilibrium at room temperature, and even intermediate temperatures.

CONCLUSIONS

Of course, the Cr-Ni binary phase diagram was already well known. But real alloys with compositions taken in the chromium-rich half diagram have almost never been elaborated and characterized, notably for very high Cr contents. The present work brought morphology information concerning the present phases, what software as Thermo-Calc is not able to bring. However, inversely the calculations carried out with Thermo-Calc allowed understanding then describing the development of the observed microstructures even if they are not homogeneous or stable (Ni segregation towards the boundaries of chromium-phase grains, fractions and composition more typical of high temperature than of room temperature). They also demonstrated that the observed microstructures of the as-cast alloys are far from the equilibrium at a future service high temperature, and then that volume fractions may evolves in use in addition to possible morphology evolution. If calculations gave useful indications to understand how the observed microstructures formed during solidification as well as during the subsequent cooling, they showed that the theoretical microstructures are also strongly dependent on temperature. But the elaboration's results also showed that such transformations may be also rather slow in this system.

In the mechanical field the imbricated microstructures of the CN3 and CN4 alloys, and potentially of the CN2 alloy if its microstructure can develop with two phases for slower cooling rates, guaranteeing a reinforcement of the highly refractory but maybe a little weak ferritic chromium phase by the stronger Cr-saturated compact austenitic nickel may be favourable. In this way the several of these alloys may represent very interesting bases for more complex alloys with additional strengthening particles.

To finish concluding one can think that elaboration by casting of so refractory alloys, which was here successful for these small ingots, will also induce difficulties for realizing bigger pieces, which are to be taken into account.

REFERENCES

[1] A.Defrance; Techniques de l'Ingénieur, Paris, **2245**, **(1998)**.

[2] D.R.Lide; Handbook of Chemistry and Physics 90th edition, CRC Press Inc, **(2009)**.

[3] P.T.B.Shaffer; Plenum press handbooks of high-temperature materials, Materials Index, Plenum Press, New York, **1**, **(1964)**.

[4] P.Kofstad; High temperature corrosion, Elsevier applied science, London, **(1988)**.

[5] C.T.Sims, W.C.Hagel, The Superalloys; John Wiley & Sons, New York, **(1972)**.

[6] E.F.Bradley, Superalloys; A technical guide, ASM International, Metals Park, **(1988)**.

[7] M.J.Donachie, S.J.Donachie; Superalloys, A Technical Guide – 2nd Edition', ASM International, Materials Park, **(2002)**.

[8] D.J.Young; 'High temperature oxidation and corrosion of metals', Elsevier, Amsterdam, **(2008)**.

[9] P.Berthod, L.Aranda, C.Vébert, S.Michon; Calphad, **28**, 159-166 **(2004)**.

[10] P.Berthod, S.Michon, L.Aranda, S.Mathieu, J.C.Gachon; Calphad, **27**, 353-359 **(2003)**.

[11] P.Berthod, Y.Hamini, L.Aranda, L.Héricher; Calphad, **31**, 351-360 **(2007)**.

[12] P.Berthod, Y.Hamini, L.Héricher, L.Aranda; Calphad, **31**, 361-369 **(2007)**.

[13] Thermo-Calc version N: "Foundation for Computational Thermodynamics" Stockholm, Sweden, Copyright, **(1993, 2000)**.